Contribution of Postsynaptic GluD2 to Presynaptic R-type Ca^{2+} Channel Function, Glutamate Release and Long-Term Potentiation at Parallel Fiber to Purkinje Cell Synapses

Manami Yamashita[1], Shin-ya Kawaguchi[1,2] and Tomoo Hirano[1]

[1] Department of Biophysics, Graduate School of Science, Kyoto University, Sakyo-ku, Kyoto 606-8502, Japan

[2] Graduate School of Brain Science, Doshisha University, Kizugawa, Kyoto 619-0225, Japan

Correspondence should be addressed to: T. Hirano
Department of Biophysics, Graduate School of Science, Kyoto University, Sakyo-ku, Kyoto 606-8502, Japan
e-mail; thirano@neurosci.biophys.kyoto-u.ac.jp
tel; 81-75-753-4237
fax; 81-75-753-4229

Conflict of interest notification

We declare no conflict of interest.

Abstract

Glutamate-receptor-like molecule delta2 (GluD2) is selectively expressed on the postsynaptic membranes at parallel fiber to Purkinje cell (PF-PC) synapses in the cerebellum. GluD2 plays critical roles not only in postsynaptic long-term depression but also in the induction of presynaptic differentiation through trans-synaptic interaction with neurexin. However, how GluD2 influences the presynaptic function remains unknown. Here, effects of the deletion of postsynaptic GluD2 on the presynaptic properties were studied focusing on the paired pulse ratio (PPR) of two consecutive EPSC amplitudes, which was larger in GluD2 knockout mice. The PPR difference remained even if saturation of glutamate binding to postsynaptic receptors was suppressed, confirming the presynaptic difference between the genotypes. We then explored the possibility that presynaptic voltage-gated Ca^{2+} channels (VGCCs) are affected in GluD2 knockout mice. Application of selective blockers for specific VGCCs indicated that R-type, but not P/Q- or N-type VGCC, was affected in the mutant mice. Furthermore, presynaptic long-term potentiation (LTP) at PF-PC synapses, which requires R-type VGCC, was impaired in GluD2 knockout mice. These results suggest that GluD2 deletion impairs presynaptic R-type VGCC, resulting in decreased release of synaptic vesicles, and also in the impairment of presynaptic LTP at PF-PC synapses.

Key words

GluD2, R-type voltage-gated calcium channel, cerebellum, parallel fiber, Purkinje cell, presynaptic plasticity

Introduction

Purkinje cells (PCs), which send the sole output from the cerebellar cortex, receive two types of excitatory synaptic inputs, one from parallel fibers (PFs) and the other from a climbing fiber (CF) coming from an inferior olivary nucleus. PF- PC synapses are the most abundant type of synapse in the mammalian central nervous system [1]. At PF-PC synapses, glutamate-receptor-like molecule delta2 (GluD2) is selectively expressed on the postsynaptic membrane [2]. GluD2 has been classified as an ionotropic glutamate receptor subunit based on amino acid sequence homology, although it shows neither glutamate binding nor ion channel function [3-8]. In GluD2 knockout mice, postsynaptic long-term depression (LTD) and motor learning are impaired, and the number of PF-PC synapses is reduced [9]. Further studies revealed the involvement of the intracellular C-terminal domain of GluD2 in LTD [10-13]. On the other hand, more recent studies demonstrated that postsynaptic GluD2 induces the differentiation of PF presynaptic terminals [14-16]. The flap loop in the extracellular N-terminal domain of GluD2 binds to cerebellin precursor protein (Cbln) secreted from PFs [17], and Cbln binds to neurexin on the presynaptic membrane of PFs [15, 18]. The GluD2-Cbln-neurexin interactions contribute to the formation, maturation and/or maintenance of PF-PC synapses.

Thus, GluD2 might influence the function of PF presynaptic terminals through the trans-synaptic interaction of Cbln and neurexin. Previous studies showed that the paired pulse ratio (PPR) of the amplitudes of two consecutive EPSCs is larger in GluD2-deficient mice than in wild-type mice [9, 14]. PPR has been shown to be correlated with the presynaptic release probability of synaptic vesicles at various synapses [19, 20], although postsynaptic saturation of transmitter binding to receptors

can also influence PPR in some cases [21, 22]. It has been reported that presynaptic neurexin influences the presynaptic release probability by regulating voltage-gated Ca^{2+} channels (VGCCs) [23, 24]. The VGCCs in PF presynaptic terminals consist of P/Q-, N-, and R-type VGCCs [25, 26]. Here, we examined the possibility that GluD2 controls VGCC(s) through interaction with neurexin and thereby supports the presynaptic release process. We show that the contribution of R-type VGCC to the release was negligible in GluD2 knockout mice. We also demonstrate that the presynaptic long-term potentiation (LTP), which depends on R-type VGCC [26], was abrogated in the mutant mice.

Materials and Methods

Sagittal cerebellar slices (250 μm thickness) were prepared from wild-type and GluD2 knockout ICR mice of either sex after decapitation [9, 14] at P14-P18. A PC was whole-cell voltage-clamped with a patch pipette (2-4 MΩ) filled with a K-gluconate based internal solution consisting of (in mM) 120 K-gluconate, 9 KCl, 3.48 $MgCl_2$, 10 HEPES, 4 NaCl, 17.5 sucrose, 4 Mg-ATP (Sigma-Aldrich, St. Louis) and 0.4 Na-GTP (Sigma-Aldrich) adjusted to pH 7.3 with KOH at room temperature (21-24 °C) [27]. The slices were continuously perfused with Krebs' solution containing (in mM) 124 NaCl, 1.8 KCl, 1.24 KH_2PO_4, 1.3 $MgCl_2$, 2.5 $CaCl_2$, 26 $NaHCO_3$ and 10 glucose oxygenated with 95% O_2 and 5% CO_2 at 21-24°C. Bicuculline (20 μM, Tocris Cookson, Bristol, UK) was added to suppress inhibitory postsynaptic currents. γ-D-Glutamylglycine (2 mM, DGG, Tocris Cookson), $NiCl_2$ (500 μM, Nacalai Tesque, Kyoto, Japan), ω-Agatoxin IVA (200 nM, AgTx, Peptide Institute, Osaka, Japan), ω-Conotoxin GVIA (500 nM, CgTx, Peptide Institute) or SNX-482 (500 nM, SNX, Peptide Institute), was applied to the bath

solution in some experiments. In the experiments examining the effects of SNX, 8-Cyclopentyl-1,3-dipropylxanthine (DPCPX, 5 μM, Tocris Cookson), (2S)-(+)-5,5-Dimethyl-2-morpholineacetic acid (SCH50911, 2 μM, Tocris Cookson) and *N*-(Piperidin-1-yl)-5-(4-iodophenyl)-1-(2,4-dichlorophenyl)-4-methyl-1*H*-pyrazole-3-carboxamide (AM251, 2 μM, Tocris Cookson) were added to block adenosine A1 receptor, $GABA_B$ receptor and cannabinoid CB1 receptor, respectively [26, 28-30]. Ionic currents were recorded with an EPC-10 amplifier (HEKA Elektronik, Lambrecht, Germany), and the signal was filtered at 2.9 kHz and digitized at 10 kHz. The membrane potential was held at –70 mV or –80 mV after compensation of the liquid junction potential. The data were discarded if the series or input resistance changed by > 20 % or the latter became < 100 MΩ. The PF-EPSCs were induced by 0.5 ms electrical stimulation of 5-15 V through a glass pipette in the molecular layer at 0.1 or 0.2 Hz. The intensity of stimulation was adjusted so that the amplitude of the first EPSC became 100-300 pA in each experiment, in order to reduce the error caused by the series resistance and also to keep good space-clamp conditions, unless otherwise stated. PPR at each interval was calculated from 3 recordings of paired EPSCs in a PC. The presynaptic LTP was induced by 30 sec, 4 Hz conditioning stimulation of PFs [31, 32]. All data were expressed as mean ± SEM. Two-way ANOVA, Dunnett test, or Student's t-test was used for statistical analyses. We regarded a difference as significant when p was < 0.05.

All experimental procedures were performed in accordance with the guidelines regarding care and use of animals for experimental procedures of the National Institutes of Health, U.S.A., and Kyoto University, and approved by the local committee for handling experimental animals in the Graduate School of Science, Kyoto University.

Results

Presynaptic change in GluD2 knockout mice increases PPR

We first confirmed that PPR was different at PF-PC synapses between wild-type and GluD2 knockout ICR mice (Figure 1ab, circles). PFs were stimulated twice with an interval of 10, 20, 50, 100 or 200 ms, and the amplitude of the second EPSC divided by that of the first EPSC was calculated as PPR. PPR was significantly different between the genotypes ($p < 0.001$, ANOVA). PPR with an interval of 50 ms was 1.69 ± 0.03 in wild-type mice ($n = 58$) and 2.04 ± 0.05 in the knockout mice ($n = 65$).

PPR has been reported to be a parameter related to the presynaptic release process [19, 20]. It has also been shown that the postsynaptic receptor availability has a significant influence on PPR in some cases [21, 22]. At PF-PC synapses saturation of glutamate binding to postsynaptic α-amino-3-hydroxy-5-methyl-4-isoxazole-propionate type ionotropic glutamate receptor (AMPAR) during the first EPSC might be negligible in a physiological condition, whereas some saturation occurs during the second EPSC in certain conditions [22, 33]. Recent immunohistological staining of AMPAR showed more intense signals in the cerebellar molecular layer of GluD2 knockout mice than in that of wild-type mice [34]. This finding raised a possibility that the number and/or distribution of AMPARs at PF-PC synapses and consequently the postsynaptic saturation during the second EPSC might be different between the two genotypes.

We evaluated the postsynaptic contribution to the PPR difference using DGG, a low-affinity competitive antagonist for AMPAR, in order to suppress the saturation of glutamate binding to AMPAR [22]. Application of 2 mM DGG decreased the amplitude of EPSCs in both wild-type mice (40.0 ± 1.8 %, $n = 5$, $p = 0.009$, Student's t-test) and GluD2 knockout mice (35.8 ± 3.0 %, $n = 5$, $p < 0.001$) (Supplemental Figure 1a,b).

Importantly, PPR was still significantly different between the two genotypes even if the postsynaptic saturation was suppressed by DGG ($p < 0.001$, ANOVA) (Figure 1a,b). In the presence of DGG, PPR at 50 ms was 2.06 ± 0.12 (n = 9) in wild-type mice, and 2.54 ± 0.12 (n = 9) in GluD2 knockout mice. These values were significantly larger than those without DGG (+/+, $p < 0.001$, -/-, $p = 0.002$, Dunnett test). Thus, the different availability of postsynaptic AMPAR alone cannot explain the difference of PPR between the genotypes. Taken together, our data suggest that in GluD2 knockout mice, PPR is larger probably because the initial release probability is lower.

PPR dependence on $[Ca^{2+}]_o$

The effects of DGG on the EPSC amplitude and PPR suggested that the presynaptic release process was altered in GluD2 knockout mice. In order to obtain some insights into the mechanism differentiating the presynaptic release machinery between the genotypes, we altered $[Ca^{2+}]_o$ to change the release probability which depends on the amplitude of Ca^{2+} influx. When $[Ca^{2+}]_o$ was increased from 1 mM to 2.5 and 4 mM, the amplitudes of the first EPSC in a PC increased to 235 ± 26 % (+/+) and 250 ± 36 % (-/-), and 383 ± 36 % (+/+) and 368 ± 59 % (-/-), respectively (n = 5 for each) (Supplemental Figure 2). These results were similar to previously reported results [22], and confirmed that presynaptic release probability is highly dependent on $[Ca^{2+}]_o$.

PPR was larger in 1 mM $[Ca^{2+}]_o$ (+/+, 2.64 ± 0.10 at 50 ms, n = 9, $p < 0.001$; -/-, 2.57 ± 0.16, n = 6, $p = 0.009$, Dunnett test, Figure 2a) and smaller in 4 mM $[Ca^{2+}]_o$ (+/+, 1.22 ± 0.04, n = 9, $p < 0.001$; -/-, 1.27 ± 0.08, n = 6, $p < 0.001$, Figure 2b) than in 2.5 mM $[Ca^{2+}]_o$, suggesting that PPR depends on the amplitude of Ca^{2+} influx. In both of these conditions, the PPR difference between the genotypes was not significant (1 mM $[Ca^{2+}]_o$,

$p = 0.87$; 4 mM $[Ca^{2+}]_o$, $p = 0.40$, ANOVA). Thus, the PPR difference was apparent only at an intermediate $[Ca^{2+}]_o$ (2.5 mM).

It has been reported that the bindings of Ca^{2+} to its sensor for the transmitter release are cooperative [35]. The Ca^{2+}-sensitivity of transmitter release is small in low $[Ca^{2+}]_i$ [36]. In such a condition, even if there is a slight difference in the Ca^{2+}-dependence of transmitter release between the genotypes, it might be difficult to detect it. Therefore, the PPR difference might become insignificant in 1mM $[Ca^{2+}]_o$. On the other hand, in higher $[Ca^{2+}]_o$ (4 mM), the release probability at the first stimulation might be high and its increase at the second stimulation might be limited, or postsynaptic glutamate binding to AMPAR might be saturated [22]. One or both of these factors seem to make PPR small in both genotypes and the PPR difference negligible in 4 mM $[Ca^{2+}]_o$. It seems that the PPR difference between the genotypes is apparent only at intermediate $[Ca^{2+}]_o$, where the Ca^{2+}-sensitivity of transmitter release is large.

P/Q- and N-type VGCC contribute to presynaptic release similarly in the two genotypes

Next, we attempted to clarify which specific presynaptic molecule was affected by GluD2 knockout and contributed to the lower presynaptic release probability. GluD2 mediates synaptic formation between PFs and a PC by interacting with presynaptic neurexin through Cbln [15, 18]. Neurexin participates in the regulation of synaptic transmission by affecting VGCCs in presynaptic terminals [23, 24]. Considering these reports together with the above results suggesting decreased presynaptic release in GluD2 knockout mice, we hypothesized that VGCC might be affected by the GluD2-ablation. There are P/Q-, N-, and R-type VGCCs in PF presynaptic terminals [25, 26]. Therefore, we performed experiments using specific blockers of each type of VGCC

to examine whether any of these VGCCs were altered by GluD2 knockout.

A P/Q-type VGCC blocker, ω-agatoxin IVA (200 nM, AgTx), clearly reduced the amplitude of evoked EPSC (+/+, 9.2 ± 1.7 %, n = 5, $p < 0.001$; -/-, 9.6 ± 2.8 %, n = 5, $p < 0.001$, Student's t-test), and enhanced PPR in both genotypes (+/+, 2.14 ± 0.10 at 50 ms, n = 9, $p < 0.001$; -/-, 2.45 ± 0.19, n = 9, p = 0.017, Dunnett test) (Figure 3a-d). Thus, P/Q-type VGCC made a large contribution to the transmitter release from PF presynaptic terminals, as reported previously [25, 26]. There was no significant difference in PPR between the genotypes after blockade of P/Q-type VGCC (p = 0.34, ANOVA). We would like to note that these results do not mean that a difference in P/Q-type VGCC causes the PPR difference between the genotypes. The Ca^{2+}-sensitivity of transmitter release is low when $[Ca^{2+}]_i$ does not reach a high value. Similarly to the results in 1 mM $[Ca^{2+}]_o$ (Figure 2a), when Ca^{2+} influx is largely suppressed by AgTx, a slight difference in the Ca^{2+}-dependence of transmitter release might not have been detected.

ω-conotoxin GVIA (500 nM, CgTx), an N-type VGCC blocker, slightly reduced the EPSC amplitude (+/+, 78.5 ± 2.2 %, n = 6, p = 0.047; -/-, 78.7 ± 2.9 %, n = 4, p = 0.034, Student's t-test), and enhanced PPR in both genotypes (+/+, 2.04 ± 0.11 at 50 ms, n = 9, p = 0.001; -/-, 2.31 ± 0.11, n = 9, p = 0.048, Dunnett test) (Figure 3e-h). PPR remained larger in the mutant mice than in wild-type mice in the presence of CgTx (p = 0.012, ANOVA). Thus, N-type VGCC makes a relatively minor contribution to the transmitter release in both genotypes.

R-type VGCC is non-functional in GluD2 knockout mice

In contrast, blockade of R-type VGCC clearly affected the PPR difference between the genotypes. Extracellular application of Ni^{2+} (500 μM), which blocks R-type VGCC,

slightly reduced the amplitude of evoked EPSC (77.6 ± 4.7 %, n = 5, p = 0.045, Student's t-test) and enhanced PPR (1.88 ± 0.06 at 50 ms, n = 12, p = 0.039, Dunnett test) in wild-type mice (Figure 4a,c). On the other hand, Ni^{2+} affected neither the EPSC amplitude (104.4 ± 11.9 %, n = 5, p = 0.85) nor PPR (2.04 ± 0.11 at 50 ms, n = 10, p = 0.99) in the knockout mice (Figure 4b,d). Ni^{2+} abolished the significant PPR difference between the genotypes (p = 0.14, ANOVA).

We noticed that even in the presence of Ni^{2+}, PPR in wild-type was still somewhat smaller at intervals < 100 ms (p = 0.022, ANOVA) and thought that this difference might be due to a difference in postsynaptic saturation of glutamate binding to receptors. To examine this possibility, we next applied DGG in addition to Ni^{2+}, and found that this made the PPR difference between the genotypes negligible (p = 0.060, n = 9, ANOVA). PPR at 50 ms was 2.24 ± 0.10 in wild-type and 2.38 ± 0.10 in knockout mice (Supplemental Figure 3). These results suggest that R-type VGCC is functional in wild-type mice but not in GluD2 knockout mice, and that this difference is likely to underlie the PPR difference between the genotypes.

We next attempted to confirm that R-type VGCC is non-functional in GluD2 knockout mice using a selective but weak R-type VGCC blocker, SNX-482 (500 nM, SNX). However, no clear effects of SNX on either the EPSC amplitude or PPR were detected in either genotype. In a previous study, Myoga and Regehr [26] showed significant effects of SNX on the EPSC in the presence of a cocktail of antagonists for adenosine A1 receptor, $GABA_B$ receptor and cannabinoid (CB) 1 receptor. These receptors suppress synaptic transmission through inhibition of presynaptic VGCCs including R-type [29, 37]. Thus, the antagonists might suppress partial inhibition of R-type VGCC and make the effects of SNX clearer. We therefore examined whether SNX would change PPR only

in wild-type mice in the presence of this cocktail in order to obtain further supporting evidence for the idea that R-type VGCC is non-functional in GluD2 knockout mice.

The cocktail of antagonists by itself increased the EPSC amplitude (+/+, 144.8 ± 10.0 %, n = 5, p = 0.013; -/-, 130.7 ± 12.0 %, n = 5, p = 0.048, Student's t-test) (Supplemental Figure 4) and decreased PPR in both wild-type (1.44 ± 0.04 at 50 ms, n = 6, p = 0.007, Student's t-test) and GluD2 (1.72 ± 0.08, n = 9, p = 0.019) knockout mice as expected. PPR was significantly different between the genotypes ($p < 0.001$, ANOVA) in this condition.

Next, we applied SNX in the presence of the cocktail. SNX decreased the EPSC amplitude (78.6 ± 1.6 %, n = 5, p = 0.006, Student's t-test) and enhanced PPR (p = 0.002, n = 6, ANOVA) in wild-type mice (Figure 4e,g). In contrast, SNX affected neither the EPSC amplitude (107.6 ± 6.7 %, n = 4, p = 0.64) nor PPR (p = 0.51, n = 9) in GluD2 knockout mice (Figure 4f,h), supporting the notion that R-type VGCC is non-functional in GluD2 knockout mice. PPR at 50 ms was 1.59 ± 0.05 in wild-type and 1.65 ± 0.08 in knockout mice. SNX abolished the significant PPR difference between the genotypes (p = 0.30, ANOVA). These results together suggest that R-type VGCC contributes to the transmitter release only in wild-type mice, and that R-type VGCC is non-functional or not expressed at PF terminals in GluD2 knockout mice, which contributes to the lower release probability and higher PPR.

Impairment of R-type VGCC-dependent presynaptic LTP in GluD2 knockout mice

It was recently reported that R-type VGCC is involved in presynaptic LTP at PF-PC synapses [26]. Considering this information and our results suggesting that presynaptic R-type VGCC is non-functional in GluD2 knockout mice, we thought that presynaptic

LTP might be affected in the knockout mice. Thus, we examined whether conditioning stimulation (4 Hz, 120 pulses) could induce presynaptic LTP in GluD2 knockout mice or not.

The conditioning stimulation increased the EPSC amplitude in wild-type mice (at 30 min, 163.3 ± 17.1 %, n = 5, p = 0.021, Student's t-test) (Figure 5a). We also found that PPR with a 50 ms interval was significantly decreased after the conditioning (before 1.70 ± 0.04, after 26-30 min 1.47 ± 0.07, Student's t-test, p = 0.023) (Figure 5b), supporting the notion that the LTP is caused by a presynaptic change. In contrast, the conditioning stimulation failed to increase the EPSC amplitude in GluD2 knockout mice (108.2 ± 8.5 %, n = 5, p = 0.39) (Figure 5a). PPR was also not altered by the conditioning stimulation in the mutant mice (before 1.96 ± 0.02, after 2.02 ± 0.15, p = 0.59) (Figure 5b). These results suggest that reduced Ca^{2+} influx through R-type VGCC abrogates the LTP induction.

It might be possible that the reduced Ca^{2+} influx to presynaptic terminals irrespective of the route suppressed the LTP induction. To address this possibility, we examined whether increased Ca^{2+} influx to presynaptic terminals in higher $[Ca^{2+}]_o$ could rescue presynaptic LTP in GluD2 knockout mice. LTP was not induced in GluD2 knockout mice in 3 mM $[Ca^{2+}]_o$ (98.4 ± 7.0 %, n = 4, p = 0.83, Student's t-test), while LTP was successfully induced in wild-type mice (143.7 ± 9.9 %, n = 4, p = 0.021) (Figure 6a). The conditioning stimulation was also applied in 4 mM $[Ca^{2+}]_o$. In this condition, LTP was not induced in either genotype (+/+, 105.6 ± 14.3 %, n = 5, p = 0.70; -/-, 90.3 ± 7.5 %, n = 5, p = 0.46) (Figure 6b). In 4 mM $[Ca^{2+}]_o$, the presynaptic release machinery might be almost fully used, and there might be no capacity to increase the presynaptic release further. Thus, increased Ca^{2+} influx in higher $[Ca^{2+}]_o$ did not rescue LTP in GluD2

knockout mice, which suggests that Ca^{2+} in microdomains near R-type VGCCs is critical for presynaptic LTP inductions as suggested by Myoga and Regehr [26].

Finally, we addressed whether an intracellular process downstream of the Ca^{2+} influx through R-type VGCC leading to the LTP induction might be affected in the knockout mice or not. Previous studies showed that forskolin, an activator of adenylyl cyclase, increases the amplitude of evoked EPSC at PF-PC synapses and prevents the induction of presynaptic LTP [26, 38]. Forskolin potentiates the synaptic transmission without changing presynaptic Ca^{2+} influx, and enhances the frequency but not the size of miniature EPSCs [39], indicating that forskolin enhances the synaptic transmission primarily via a presynaptic process independent of Ca^{2+} influx. Thus, an increase in $[cAMP]_i$ might be a process downstream of $[Ca^{2+}]_i$ increase in the LTP induction. We found that forskolin increased the EPSC amplitude (at 9-10 min, +/+, 137.7 ± 13.8 %, n = 5, p = 0.038; -/-, 143.3 ± 17.6 %, n = 6, p = 0.044, Student's t-test) and reduced PPR with an interval of 50 ms (+/+, before, 1.62 ± 0.11, after 9-10 min, 1.29 ± 0.06, p = 0.038; -/-, before, 1.96 ± 0.08, after, 1.42 ± 0.08, p < 0.001, Student's t-test) in both genotypes (Figure 6c). There was no significant difference between the genotypes either in the increase in EPSC amplitude (p = 0.81) or in the decrease in PPR (p = 0.26, Student's t-test). Therefore, steps downstream of the $[cAMP]_i$ increase in the potentiation cascade of presynaptic release seem not to be affected by deletion of GluD2.

Discussion

Pre- and postsynaptic regulation by GluD2

GluD2 is selectively expressed on the postsynaptic membrane at PF-PC synapses and is required for cerebellar LTD [9, 40], which has been considered to be a critical

mechanism for motor learning [41, 42]. This LTD is expressed at the postsynaptic membrane as a decrease in the number of postsynaptic AMPARs [43]. GluD2 is also involved in synaptic formation through interaction with presynaptic neurexin and secreted Cbln [15, 16]. Thus, GluD2 plays roles in organizing both presynaptic and postsynaptic sites through its extracellular and intracellular domains, respectively [7, 8].

Both pre- and postsynaptic mechanisms contribute to paired pulse facilitation of EPSC amplitudes, although the preponderance of the evidence suggests that the former is the main determinant of PPR [20, 44, 45]. GluD2 knockout mice show an increase in the number of postsynaptic AMPARs at PF-PC synapses [34], which led us to examine whether the contribution of postsynaptic saturation to PPR was different between the wild-type and GluD2 knockout genotypes. When DGG was used to suppress the saturation of glutamate binding to postsynaptic AMPAR [22], we found that even in the presence of DGG, PPR was still larger in GluD2 knockout mice, suggesting that there are some presynaptic changes in these mice.

Presynaptic VGCC is affected by GluD2 knockout

Multiple mechanisms directly or indirectly modulate the function of presynaptic VGCCs and regulate synaptic transmission [46, 47]. P/Q- and N-type VGCCs mainly contribute to the synaptic transmission in the central nervous system, and have different gating and recruitment mechanisms [46, 48]. For example, endocannabinoid suppresses the N-, P/Q- and R-type VGCCs differently in presynaptic terminals [37]. At rat PF presynaptic terminals, the contribution of Ca^{2+} increase through P/Q-type VGCC is the largest, followed by that through N- and R-type VGCCs [26]. We confirmed that the

contributions of N- and R-type VGCCs were similar and limited in wild-type mice, and then demonstrated that R-type VGCC was non-functional in GluD2 knockout mice. We also showed that the effects of blocking P/Q- or N-type VGCC on EPSC amplitude were similar between these two genotypes. These results suggest that Ca^{2+} influx through P/Q- and N-type VGCC, and their coupling to glutamate release are not affected by GluD2 knockout, and that only R-type VGCC becomes non-functional. A slot hypothesis for presynaptic VGCCs proposes that there are different kinds of VGCC slots in presynaptic terminals [49, 50]. Slots preferring P/Q-type VGCC and those preferring N-type VGCC were reported. There might also be slots preferring R-type VGCC in PF presynaptic terminals, which might be affected by GluD2 deletion.

Ca^{2+} microdomains near R-type, but not those around P/Q- or N- type VGCC, control the induction of presynaptic LTP at rat PF-PC synapses [26]. Our finding of impaired presynaptic R-type VGCC in PF terminals of GluD2 knockout mice raised the possibility that presynaptic LTP might also be affected. As expected, we found that LTP was suppressed in GluD2 knockout mice. Furthermore, we also demonstrated that LTP failure was not rescued by an increase in $[Ca^{2+}]_o$, suggesting that not ambient Ca^{2+} in the presynaptic terminal but Ca^{2+} in the microdomain around R-type VGCC is critical for the LTP induction. Thus, R-type-preferring slots in PF terminals might be located close to signaling molecules involved in presynaptic LTP. In addition, we found that the effects of forskolin were similar between the genotypes. Forskolin increases $[cAMP]_i$ through activation of adenylyl cyclase, enhances the presynaptic release and prevents the LTP induction at PF-PC synapses [26, 38]. Thus, the $[cAMP]_i$ increase has been a candidate downstream process of the $[Ca^{2+}]_i$ increase in LTP induction. Our results indicate that the steps downstream of the $[cAMP]_i$ increase are not affected by GluD2

knockout. Taking these facts together, we suggest that postsynaptic GluD2 deficiency impairs not only postsynaptic LTD, but also presynaptic LTP, presumably through alteration of presynaptic R-type VGCC.

Retrograde regulation of presynaptic properties

Pre- and postsynaptic coordination is brought about by interactions between membrane-bound molecules on the two sides of the synaptic cleft or through secreted messenger molecules. Correlations between pre- and postsynaptic structures and functions differ between cerebellar and hippocampal glutamatergic synapses [51]. There is evidence that a postsynaptic neuron determines presynaptic functional properties. For example, PF synapses on PCs or on cerebellar inhibitory interneurons show different presynaptic short-term plasticity [52, 53]. A trans-synaptic interaction by synaptic adhesion molecules could bridge the presynaptic release apparatus with the postsynaptic density. Postsynaptic neuroligin or leucine-rich repeat transmembrane protein contacts presynaptic neurexin, and this interaction induces the differentiation of both pre- and postsynaptic structures [54-57]. Interactions between different pairs of synaptic adhesion molecules such as neuroligin and neurexin splice isoforms might determine excitatory versus inhibitory synapse formation, and also the properties of synapses [58]. GluD2 mediates synapse formation between PFs and a PC by interacting with presynaptic neurexin through Cbln [15]. Even if GluD2 is ablated, PF synapses on a PC can be formed through neuroligin-neurexin interaction, etc. The affinity for binding between Cbln and GluD2, and that for binding between Cbln and certain types of neurexin (K_d = 16.5 nM and 0.17 nM, respectively), are higher than those for binding between various subtypes of neuroligin and neurexin (K_d = 200-600 nM) [15, 59, 60].

Thus, neurexin1β (+4), which is expressed in presynaptic terminals of PFs, seems to preferentially bind to GluD2 through Cbln rather than to neuroligin. On the other hand, in the absence of GluD2, presynaptic neurexin might bind to neuroligin. Whether neurexin binds to GluD2 or neuroligin might determine presynaptic properties. As mentioned above, the presynaptic properties of PF terminals are different depending on whether the postsynaptic neurons are PCs expressing GluD2 or inhibitory interneurons without GluD2. In addition, neurexin was reported to influence presynaptic release probability by affecting VGCCs, as described above [23, 24]. Taking all these facts together, we suggest that postsynaptic GluD2 affects presynaptic R-type VGCC through interaction with Cbln and neurexin, contributing to the transmitter release process and to formation of Ca^{2+} microdomains involved in the induction of presynaptic LTP.

Conclusion

We examined the roles of postsynaptic GluD2 in the functional regulation of presynaptic PF terminals. PPR measurement in the presence of DGG, which suppresses saturation of glutamate binding to postsynaptic AMPAR, suggested that the presynaptic release probability was lower in GluD2 knockout mice than in wild-type mice. Application of selective inhibitors for specific VGCCs revealed that the contribution of R-type, but not P/Q- or N-type, VGCC to presynaptic release was affected in the mutant mice. Furthermore, we found that the presynaptic R-type VGCC-dependent LTP was impaired in GluD2 knockout mice. Based on all these findings, we suggest that postsynaptic GluD2 deletion impairs the function of the presynaptic R-type VGCC, resulting in decreased release of synaptic vesicles, enhanced PPR, and impaired

presynaptic LTP induction.

Acknowledgments

We thank Y. Tagawa, G. Ohtsuki, and E. Nakajima for comments on the manuscript. This work was supported by a grant-in-aid for scientific research from the Ministry of Education, Culture, Sports, Science and Technology in Japan, Takeda Science Foundation, and also by Global COE program A06 of Kyoto University.

References

1. Ito M. Cerebellar circuitry as a neuronal machine. Prog Neurobiol 2006; 78: 272-303.

2. Takayama C, Nakagawa S, Watanabe M, Mishina M, Inoue Y. Light- and electron-microscopic localization of the glutamate receptor channel δ2 subunit in the mouse Purkinje cell. Neurosci Lett 1995; 188: 89-92.

3. Araki K, Meguro H, Kushiya E, Takayama C, Inoue Y, Mishina M. Selective expression of the glutamate receptor channel δ2 subunit in cerebellar Purkinje cells. Biochem Biophys Res Commun 1993; 197: 1267-76.

4. Lomeli H, Sprengel R, Laurie DJ, Köhr G, Herb A, Seeburg PH, Wisden W. The rat delta-1 and delta-2 subunits extend the excitatory amino acid receptor family. FEBS Lett 1993; 315: 318-22.

5. Schmid SM, Kott S, Sager C, Huelsken T, Hollmann M. The glutamate receptor subunit delta2 is capable of gating its intrinsic ion channel as revealed by ligand binding domain transplantation. Proc Natl Acad Sci U S A 2009; 106: 10320-5.

6. Mandolesi G, Cesa R, Autuori E, Strata P. An orphan ionotropic glutamate receptor: the δ2 subunit. Neuroscience 2009; 158: 67-77.

7. Yuzaki M. New (but old) molecules regulating synapse integrity and plasticity: Cbln1 and the δ2 glutamate receptor. Neuroscience 2009; 162: 633-43.

8. Hirano T. Glutamate-receptor-like molecule GluRδ2 involved in synapse formation at parallel fiber-Purkinje neuron synapses. Cerebellum 2012; 11: 71-7.

9. Kashiwabuchi N, Ikeda K, Araki K, Hirano T, Shibuki K, Takayama C, et al. Impairment of motor coordination, Purkinje cell synapse formation, and cerebellar long-term depression in GluRδ2 mutant mice. Cell 1995; 81: 245-52.

10. Yawata S, Tsuchida H, Kengaku M, Hirano T. Membrane-proximal region of glutamate receptor δ2 subunit is critical for long-term depression and interaction

with protein interacting with C kinase 1 in a cerebellar Purkinje neuron. J Neurosci 2006; 26: 3626-33.

11. Kohda K, Kakegawa W, Matsuda S, Nakagami R, Kakiya N, Yuzaki M. The extreme C-terminus of GluRδ2 is essential for induction of long-term depression in cerebellar slices. Eur J Neurosci 2007; 25: 1357-62.

12. Uemura T, Kakizawa S, Yamasaki M, Sakimura K, Watanabe M, Iino M, et al. Regulation of long-term depression and climbing fiber territory by glutamate receptor δ2 at parallel fiber synapses through its C-terminal domain in cerebellar Purkinje cells. J Neurosci 2007; 27: 12096-108.

13. Torashima T, Iizuka A, Horiuchi H, Mitsumura K, Yamasaki M, Koyama C, et al. Rescue of abnormal phenotypes in δ2 glutamate receptor-deficient mice by the extracellular N-terminal and intracellular C-terminal domains of the δ2 glutamate receptor. Eur J Neurosci 2009; 30: 355-65.

14. Kuroyanagi T, Yokoyama M, Hirano T. Postsynaptic glutamate receptor δ family contributes to presynaptic terminal differentiation and establishment of synaptic transmission. Proc Natl Acad Sci U S A 2009; 106: 4912-6.

15. Uemura T, Lee SJ, Yasumura M, Takeuchi T, Yoshida T, Ra M, et al. Trans-synaptic interaction of GluRδ2 and Neurexin through Cbln1 mediates synapse formation in the cerebellum. Cell 2010; 141: 1068-79.

16. Matsuda K, Miura E, Miyazaki T, Kakegawa W, Emi K, Narumi S, et al. Cbln1 is a ligand for an orphan glutamate receptor δ2, a bidirectional synapse organizer. Science 2010; 328: 363-8.

17. Kuroyanagi T, Hirano T. Flap loop of GluD2 binds to Cbln1 and induces presynaptic differentiation. Biochem Biophys Res Commun 2010; 398: 537-41.

18. Matsuda K, Yuzaki M. Cbln family proteins promote synapse formation by regulating distinct neurexin signaling pathways in various brain regions. Eur J Neurosci 2011; 33: 1447-61.

19. Debanne D, Guérineau NC, Gähwiler BH, Thompson SM. Paired-pulse facilitation and depression at unitary synapses in rat hippocampus: quantal fluctuation affects subsequent release. J Physiol 1996; 491: 163-76.

20. Hashimoto K, Kano M. Presynaptic origin of paired-pulse depression at climbing fibre-Purkinje cell synapses in the rat cerebellum. J Physiol 1998; 506: 391-405.

21. Wadiche JI, Jahr CE. Multivesicular release at climbing fiber-Purkinje cell synapses. Neuron 2001; 32: 301-13.

22. Foster KA, Crowley JJ, Regehr WG. The influence of multivesicular release and postsynaptic receptor saturation on transmission at granule cell to Purkinje cell synapses. J Neurosci 2005; 25: 11655-65.

23. Missler M, Zhang W, Rohlmann A, Kattenstroth G, Hammer RE, Gottmann K, et al. α-neurexins couple Ca^{2+} channels to synaptic vesicle exocytosis. Nature 2003; 423: 939-48.

24. Zhang W, Rohlmann A, Sargsyan V, Aramuni G, Hammer RE, Südhof TC, et al. Extracellular domains of α-neurexins participate in regulating synaptic transmission by selectively affecting N- and P/Q-type Ca^{2+} channels. J Neurosci 2005; 25: 4330-42.

25. Mintz IM, Sabatini BL, Regehr WG. Calcium control of transmitter release at a cerebellar synapse. Neuron 1995; 15: 675-88.

26. Myoga MH, Regehr WG. Calcium microdomains near R-type calcium channels control the induction of presynaptic long-term potentiation at parallel fiber to Purkinje cell synapses. J Neurosci 2011; 31: 5235-43.

27. Coesmans M, Weber JT, De Zeeuw CI, Hansel C. Bidirectional parallel fiber plasticity in the cerebellum under climbing fiber control. Neuron 2004; 44: 691-700.

28. Wall MJ, Dale N. Auto-inhibition of rat parallel fibre-Purkinje cell synapses by activity-dependent adenosine release. J Physiol 2007; 581: 553-65.

29. Dittman JS, Regehr WG. Contributions of calcium-dependent and calcium-independent mechanisms to presynaptic inhibition at a cerebellar synapse. J Neurosci 1996; 16: 1623-33.

30. Kreitzer AC, Regehr WG. Retrograde inhibition of presynaptic calcium influx by endogenous cannabinoids at excitatory synapses onto Purkinje cells. Neuron 2001; 29: 717-27.

31. Hirano T. Differential pre- and postsynaptic mechanisms for synaptic potentiation and depression between a granule cell and a Purkinje cell in rat cerebellar culture. Synapse 1991; 7: 321-3.

32. Qiu DL, Knöpfel T. An NMDA receptor/nitric oxide cascade in presynaptic parallel fiber-Purkinje neuron long-term potentiation. J Neurosci 2007; 27: 3408-15.

33. Valera AM, Doussau F, Poulain B, Barbour B, Isope P. Adaptation of granule cell to Purkinje cell synapses to high-frequency transmission. J Neurosci 2012; 32: 3267-80.

34. Yamasaki M, Miyazaki T, Azechi H, Abe M, Natsume R, Hagiwara T, et al. Glutamate receptor δ2 is essential for input pathway-dependent regulation of synaptic AMPAR contents in cerebellar Purkinje cells. J Neurosci 2011; 31: 3362-74.

35. Augustine GJ. How does calcium trigger neurotransmitter release? Curr Opin Neurobiol 2001; 11: 320-6.

36. Kochubey O, Lou X, Schneggenburger R. Regulation of transmitter release by Ca^{2+} and synaptotagmin: insights from a large CNS synapse. Trends Neurosci 2011; 34: 237-46.

37. Brown SP, Safo PK, Regehr WG. Endocannabinoids inhibit transmission at granule cell to Purkinje cell synapses by modulating three types of presynaptic calcium channels. J Neurosci 2004; 24: 5623-31.

38. Salin PA, Malenka RC, Nicoll RA. Cyclic AMP mediates a presynaptic form of LTP at cerebellar parallel fiber synapses. Neuron 1996; 16: 797-803.

39. Chen C, Regehr WG. The mechanism of cAMP-mediated enhancement at a cerebellar synapse. J Neurosci. 1997; 17:8687-94.

40. Hirano T, Kasono K, Araki K, Shinozuka K, Mishina M. Involvement of the glutamate receptor δ2 subunit in the long-term depression of glutamate responsiveness in cultured rat Purkinje cells. Neurosci Lett 1994; 182: 172-6.

41. Boyden ES, Katoh A, Raymond JL. Cerebellum-dependent learning: the role of multiple plasticity mechanisms. Annu Rev Neurosci 2004; 27: 581-609.

42. Ito M. Cerebellar long-term depression: characterization, signal transduction, and functional roles. Physiol Rev 2001; 81: 1143-95.

43. Linden DJ. The expression of cerebellar LTD in culture is not associated with changes in AMPA-receptor kinetics, agonist affinity, or unitary conductance. Proc Natl Acad Sci U S A 2001; 98: 14066-71.

44. Atluri PP, Regehr WG. Determinants of the time course of facilitation at the granule cell to Purkinje cell synapse. J Neurosci 1996; 16: 5661-71.

45. Zucker RS, Regehr WG. Short-term synaptic plasticity. Annu Rev Physiol 2002; 64: 355-405.

46. Catterall WA. Structure and regulation of voltage-gated Ca^{2+} channels. Annu Rev Cell Dev Biol 2000; 16: 521-55.

47. Tedford HW, Zamponi GW. Direct G protein modulation of Ca_V2 calcium channels. Pharmacol Rev 2006; 58: 837-62.

48. Li L, Bischofberger J, Jonas P. Differential gating and recruitment of P/Q-, N-, and R-type Ca^{2+} channels in hippocampal mossy fiber boutons. J Neurosci 2007; 27: 13420-9.

49. Cao YQ, Piedras-Rentería ES, Smith GB, Chen G, Harata NC, Tsien RW. Presynaptic Ca^{2+} channels compete for channel type-preferring slots in altered neurotransmission arising from Ca^{2+} channelopathy. Neuron 2004; 43: 387-400.

50. Cao YQ, Tsien RW. Different relationship of N- and P/Q-type Ca^{2+} channels to channel-interacting slots in controlling neurotransmission at cultured hippocampal synapses. J Neurosci 2010; 30: 4536-46.

51. Miyawaki H, Hirano T. Different correlations among physiological and morphological properties at single glutamatergic synapses in the rat hippocampus and the cerebellum. Synapse 2011; 65: 412-23.

52. Delaney AJ, Jahr CE. Kainate receptors differentially regulate release at two parallel fiber synapses. Neuron 2002; 36: 475-82.

53. Bao J, Reim K, Sakaba T. Target-dependent feedforward inhibition mediated by short-term synaptic plasticity in the cerebellum. J Neurosci 2010; 30: 8171-9.

54. Craig AM, Kang Y. Neurexin-neuroligin signaling in synapse development. Curr Opin Neurobiol 2007; 17: 43-52.

55. Südhof TC. Neuroligins and neurexins link synaptic function to cognitive disease. Nature 2008; 455: 903-11.

56. Linhoff MW, Laurén J, Cassidy RM, Dobie FA, Takahashi H, Nygaard HB, et al. An unbiased expression screen for synaptogenic proteins identifies the LRRTM protein family as synaptic organizers. Neuron 2009; 61: 734-49.

57. Ko J, Soler-Llavina GJ, Fuccillo MV, Malenka RC, Südhof TC. Neuroligins/LRRTMs prevent activity- and Ca^{2+}/calmodulin-dependent synapse elimination in cultured neurons. J Cell Biol 2011; 194: 323-34.

58. Chubykin AA, Atasoy D, Etherton MR, Brose N, Kavalali ET, Gibson JR, et al. Activity-dependent validation of excitatory versus inhibitory synapses by neuroligin-1 versus neuroligin-2. Neuron 2007; 54: 919-31.

59. Comoletti D, Flynn R, Jennings LL, Chubykin A, Matsumura T, Hasegawa H, et al. Characterization of the interaction of a recombinant soluble neuroligin-1 with neurexin-1ß. J Biol Chem 2003; 278: 50497-505.

60. Koehnke J, Jin X, Trbovic N, Katsamba PS, Brasch J, Ahlsen G, et al. Crystal structures of ß-neurexin 1 and ß-neurexin 2 ectodomains and dynamics of splice insertion sequence 4. Structure 2008; 16: 410-21.

Legends

Figure 1

PPR difference between the two genotypes. (a, b), PPR with various intervals in the absence (circles; a, n = 58, b, n = 65) or in the presence (squares; n =9 for each) of 2 mM DGG in wild-type (a) and GluD2 knockout (b) mice. Representative traces of paired EPSCs are also presented. The vertical scale is adjusted so that the first EPSC amplitudes with or without DGG become similar.

Figure 2

PPR in 1 mM (a) or 4 mM (b) $[Ca^{2+}]_o$. PPR (+/+, open circles, n = 9; -/-, filled circles, n = 6) and representative EPSC traces are presented.

Figure 3

Effects of AgTx or CgTx on the amplitude of EPSC and PPR. (a, b), Decrease of the amplitude of evoked EPSC by AgTx (200 nM) in wild-type (+/+, n = 5) (a) and in knockout (-/-,n = 5) (b) mice. Representative traces of paired EPSCs are presented. (c, d), PPR with various intervals in the absence (circles) or presence (triangle) of AgTx in wild-type (+/+, n = 9) (c) and in knockout (-/-, n = 9) (d) mice. (e, f), Suppression of amplitude of evoked EPSC by CgTx (500 nM) in wild-type (+/+, n = 6) (e) and in knockout (-/-, n = 4) (f) mice. Representative traces of paired EPSCs are presented. (g, h),

PPR with various intervals in the absence (circles) or presence (triangles) of CgTx in wild-type (+/+, n = 9) (g) and in knockout (-/-, n = 9) (h) mice. The data without AgTx or CgTx (circles) are the same as shown in Figure 1c and d, which are presented for comparison.

Figure 4

Effects of Ni^{2+} or SNX on the amplitude of EPSC and PPR. (a, b), Decrease of the amplitude of evoked EPSC by Ni^{2+} (500 μM) in wild-type (+/+, n = 5) (a) and in knockout (-/-, n = 5) (b) mice. Representative traces of paired EPSCs are presented. (c, d), PPR with various intervals in the absence (circles) or presence (triangles) of Ni^{2+}, in wild-type (+/+, n = 12) (c) and in knockout (-/-, n = 10) (d) mice. The data without Ni^{2+} (circles) are the same as shown in Figure 1c and d, which are presented for comparison. (e, f), Decrease of amplitude of evoked EPSC by SNX (500 nM) in wild-type (+/+, n = 5) (e) and knockout (-/-, n = 4) (f) mice. Representative traces of paired EPSCs are presented. (g, h), PPR with various intervals in the absence (circles) or presence (triangles) of SNX in wild-type (+/+, n = 6) (g) and in knockout (-/-, n = 9) (h) mice. (e-h), These experiments were performed in the presence of antagonists for A1, $GABA_B$ and CB1 receptors .

Figure 5

Impairment of presynaptic LTP in GluD2 knockout mice. (a), The time courses of EPSC amplitude before and after the 4 Hz, 30 sec, PF stimulation at 0 min in wild-type mice (+/+, open circles, n = 5) and in knockout (-/-, filled circles, n =5) mice. Representative traces of paired EPSCs are also presented. (b) PPR with 50 ms interval before and after the conditioning stimulation (*, $p < 0.05$).

Figure 6

(a, b), The time courses of EPSC amplitude before and after the 4 Hz, 30 sec, PF stimulation at 0 min in wild-type (+/+, open circles) and in knockout (-/-, filled circles) mice in 3 mM $[Ca^{2+}]_o$ (+/+, n = 4; -/-, n = 4)(a) or in 4 mM $[Ca^{2+}]_o$ (+/+, n = 5; -/-, n = 5) (b). (c), The time courses of EPSC amplitude before and after the application of forskolin (50 μM) in wild-type (+/+, open circles, n = 5) and in knockout (-/-, filled circles, n = 6) mice.

Supplemental Figure 1

Effects of DGG on the EPSC amplitude. (a, b), The decrease in EPSC amplitude caused by application of 2 mM DGG in wild-type (+/+, n = 5) (a) and GluD2 knockout (-/-, n = 5) (b) mice.

Supplemental Figure 2

The time courses of EPSC amplitude change when $[Ca^{2+}]_o$ was increased in wild-type (+/+, open circles, n = 5) and in knockout (-/-, filled circles, n = 5) mice.

Supplemental Figure 3

PPR with various intervals in the presence of both Ni^{2+} and DGG in wild-type (+/+, open circles, n = 9) and in knockout (-/-, filled circles, n = 9) mice.

Supplemental Figure 4

Effects of a cocktail of antagonists for A1R, $GABA_BR$ and CB1R. Application of the cocktail increased the EPSC amplitude both in wild-type (+/+, open circles, n = 5) and in knockout (-/-, filled circles, n = 5) mice.

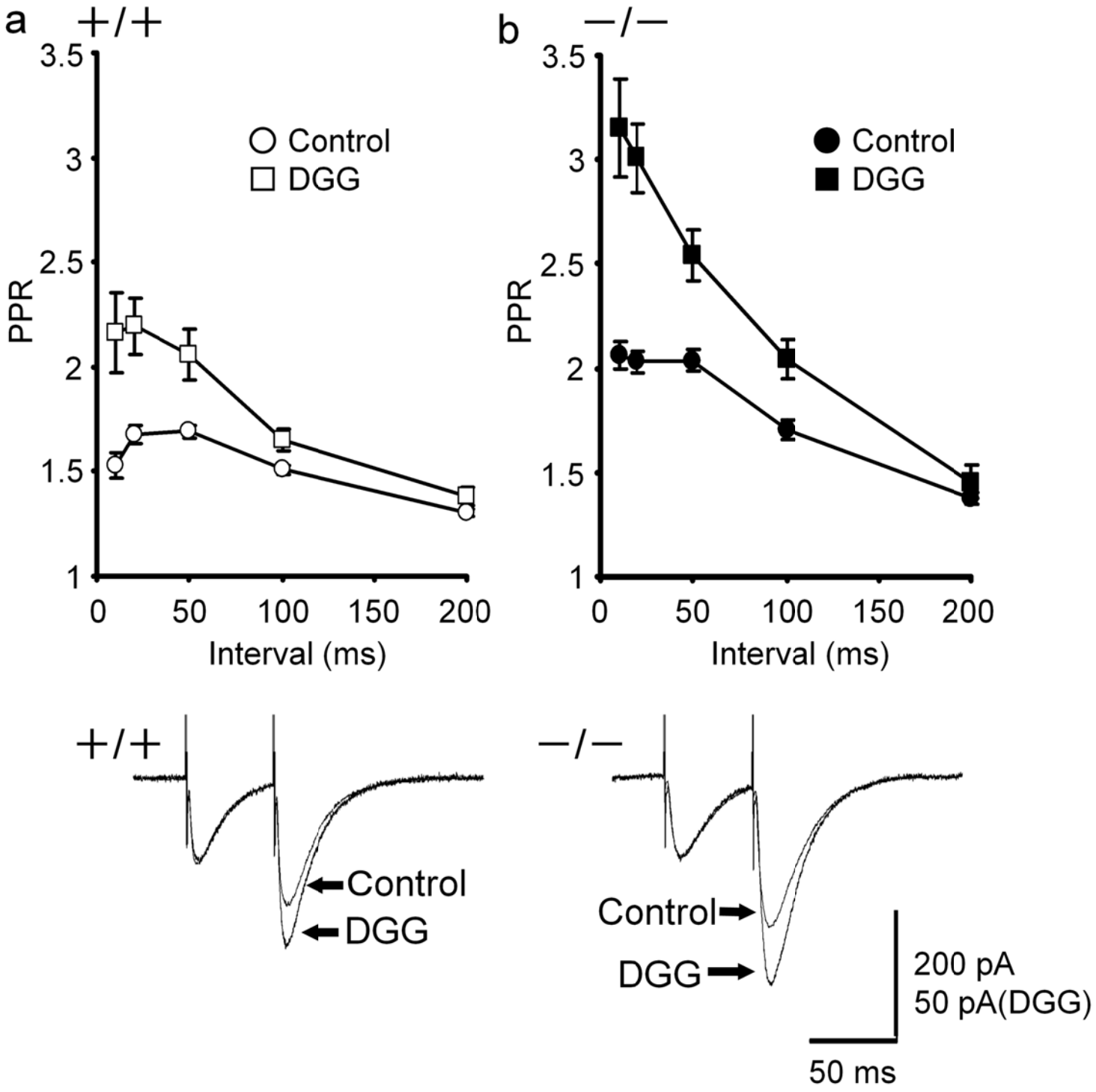
a
+/+
3.5
3
2.5
2
1.5
1
PPR
Control
DGG
0
50
100
150
200
Interval (ms)
b
−/−
3.5
3
2.5
2
1.5
1
PPR
Control
DGG
0
50
100
150
200
Interval (ms)
+/+
Control
DGG
−/−
Control
DGG
200 pA
50 pA(DGG)
50 ms

Figure 1

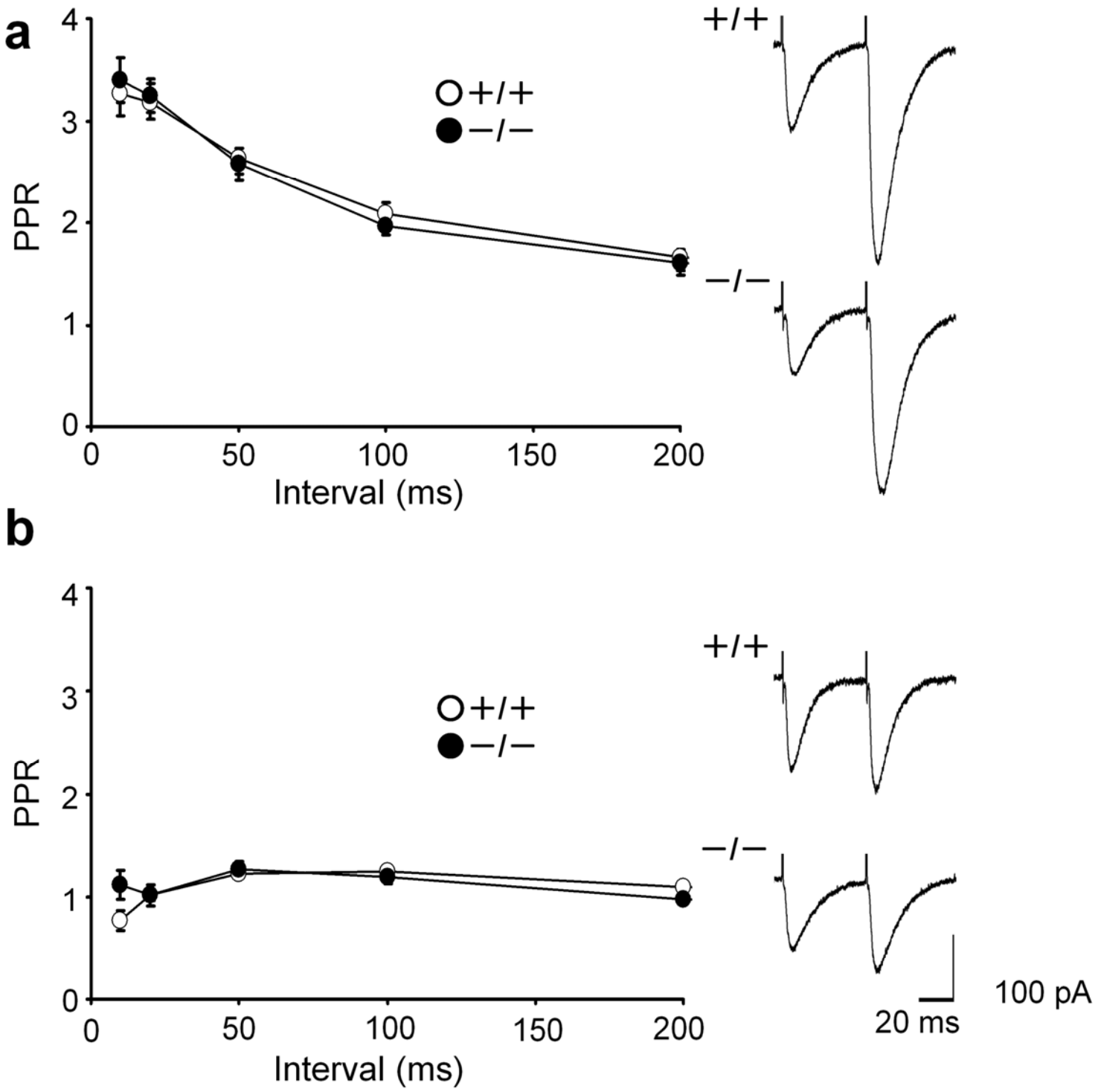

Figure 2

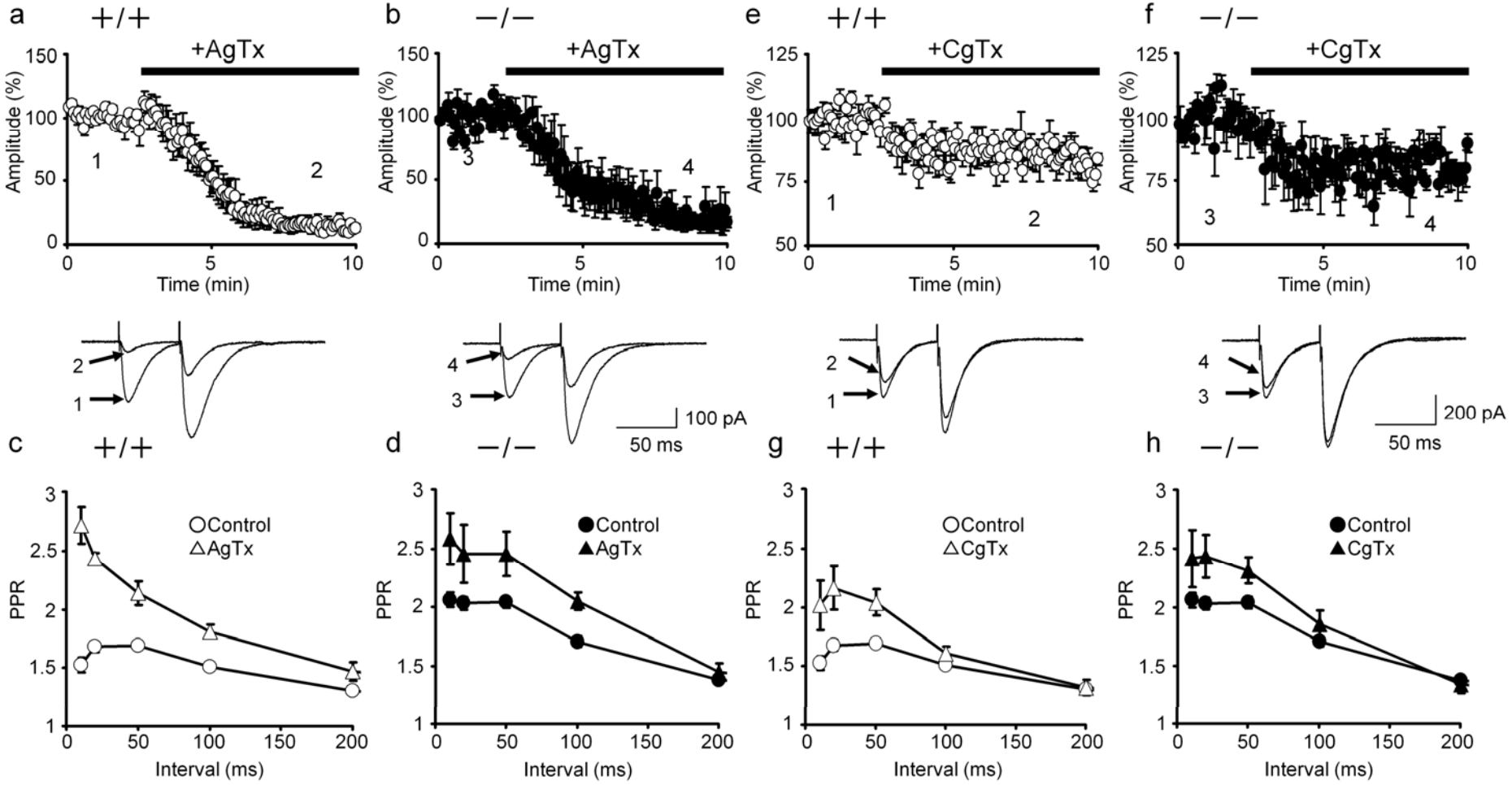
a
+/+
+AgTx
Amplitude (%)
Time (min)
b
−/−
+AgTx
e
+/+
+CgTx
f
−/−
+CgTx
100 pA
50 ms
200 pA
c
+/+
○Control
△AgTx
d
−/−
●Control
▲AgTx
g
+/+
○Control
△CgTx
h
−/−
●Control
▲CgTx
PPR
Interval (ms)

Figure 3

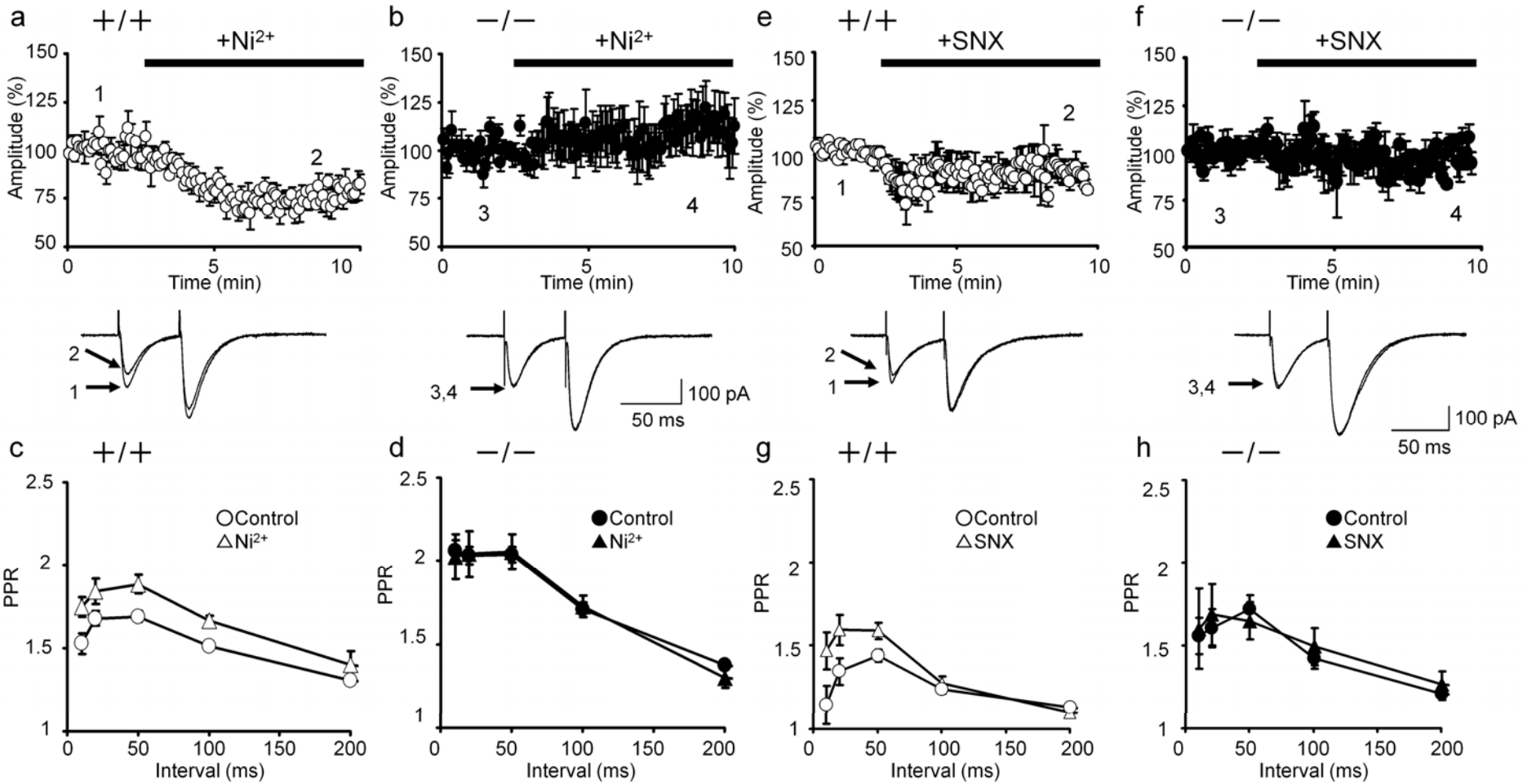
a
+/+
+Ni2+
Amplitude (%)
Time (min)
b
−/−
+Ni2+
e
+/+
+SNX
f
−/−
+SNX
100 pA
50 ms
c
+/+
○Control
△Ni2+
d
−/−
●Control
▲Ni2+
g
+/+
○Control
△SNX
h
−/−
●Control
▲SNX
PPR
Interval (ms)

Figure 4

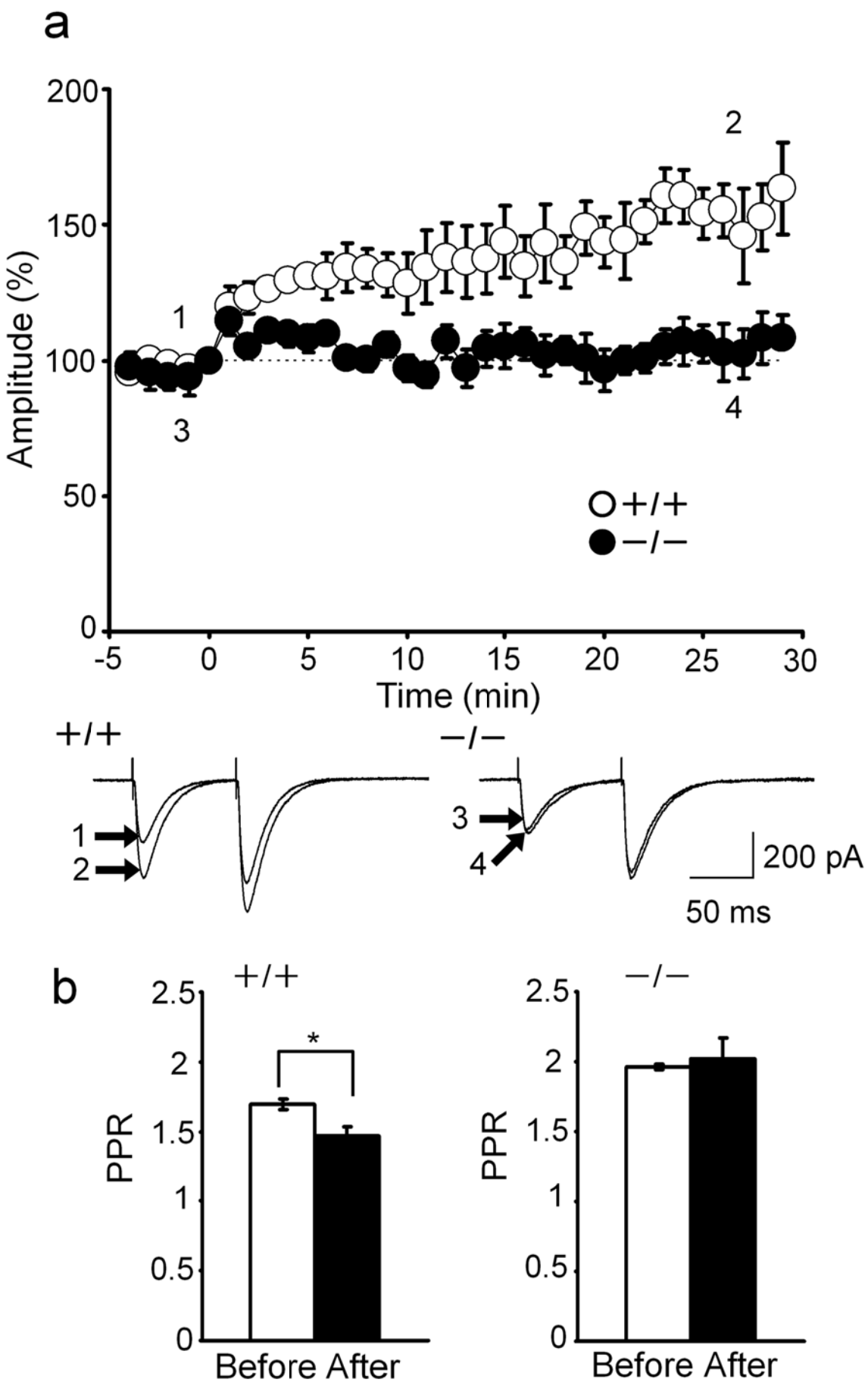
a
200
150
100
50
0
Amplitude (%)
1
2
3
4
+/+
−/−
-5
0
5
10
15
20
25
30
Time (min)
+/+
−/−
1
2
3
4
200 pA
50 ms
b
+/+
−/−
2.5
2
1.5
1
0.5
0
PPR
*
Before After
Before After

Figure 5

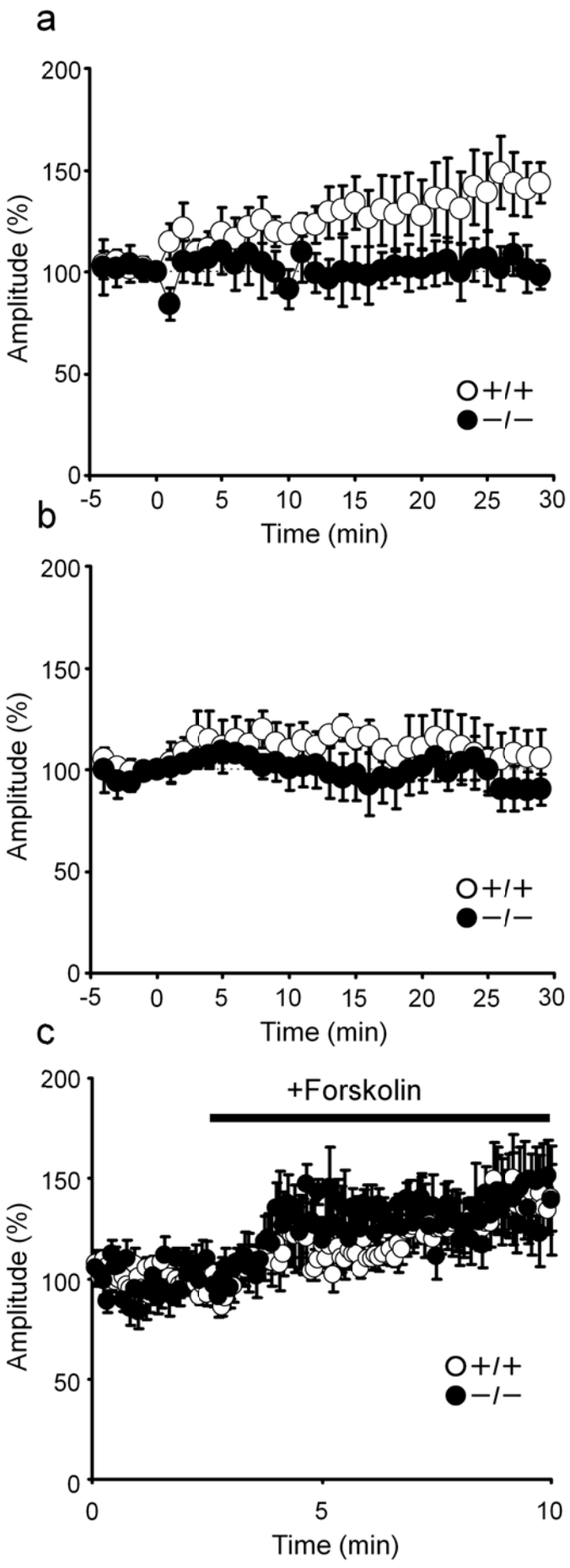
a
200
150
100
50
0
Amplitude (%)
+/+
−/−
-5
0
5
10
15
20
25
30
Time (min)
b
200
150
100
50
0
Amplitude (%)
+/+
−/−
-5
0
5
10
15
20
25
30
Time (min)
c
+Forskolin
200
150
100
50
0
Amplitude (%)
+/+
−/−
0
5
10
Time (min)

Figure 6

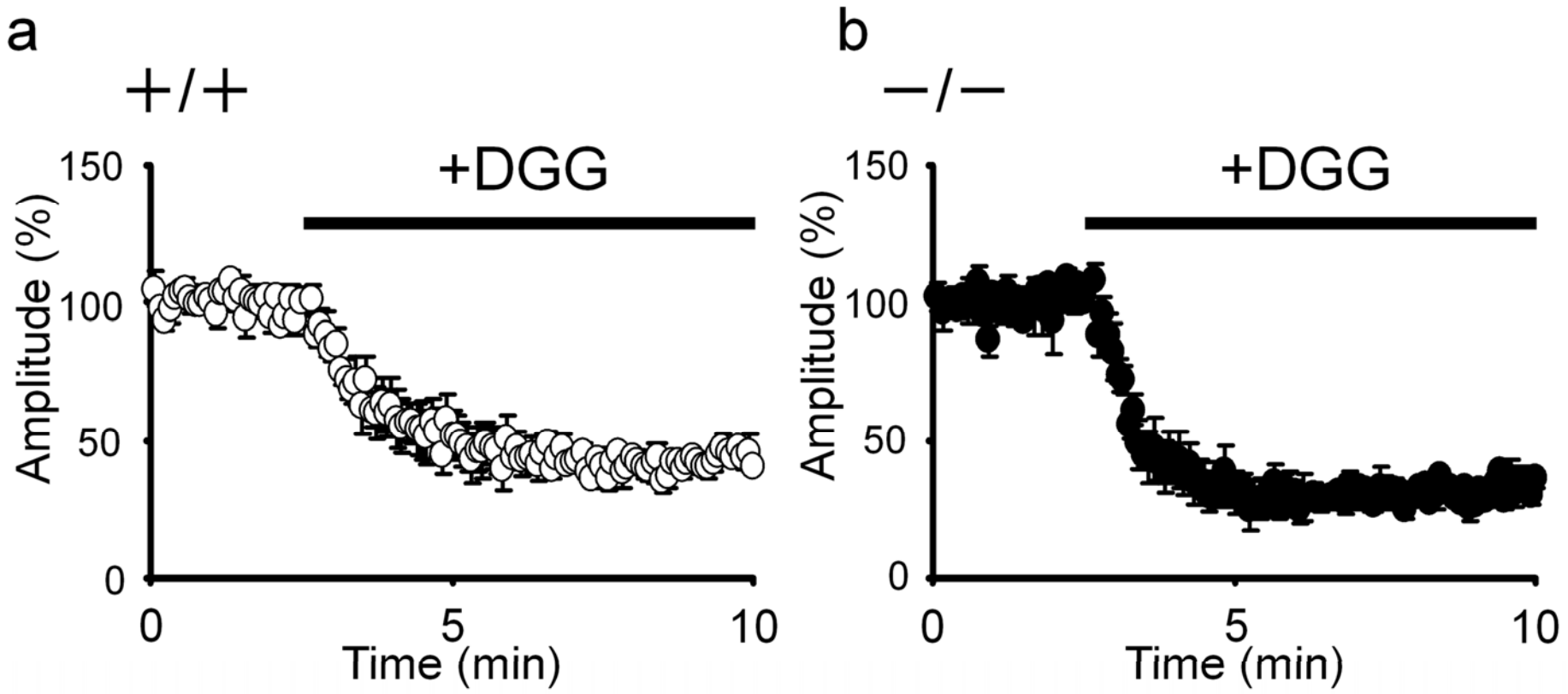

Supplemental Figure 1

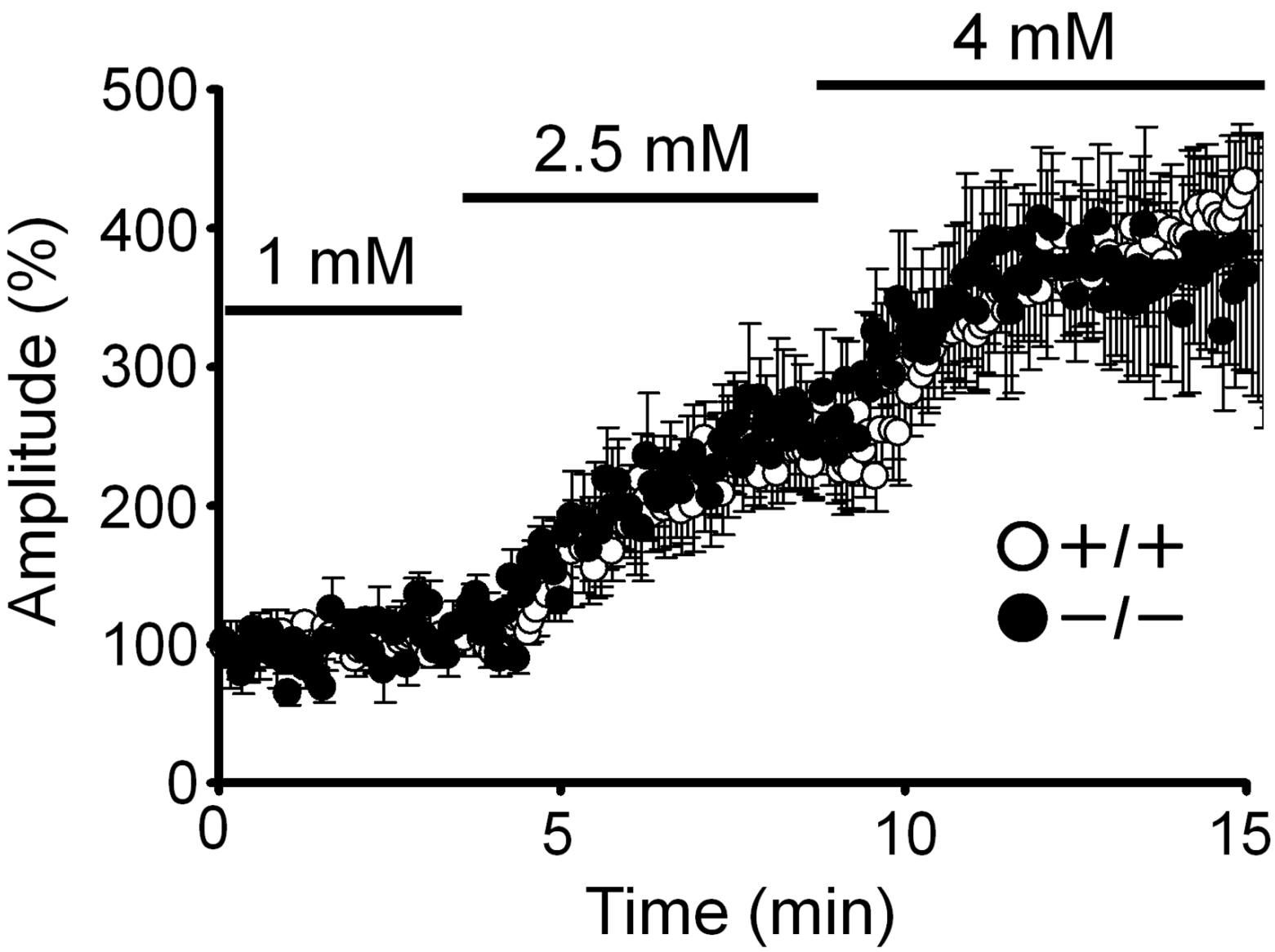

Supplemental Figure 2

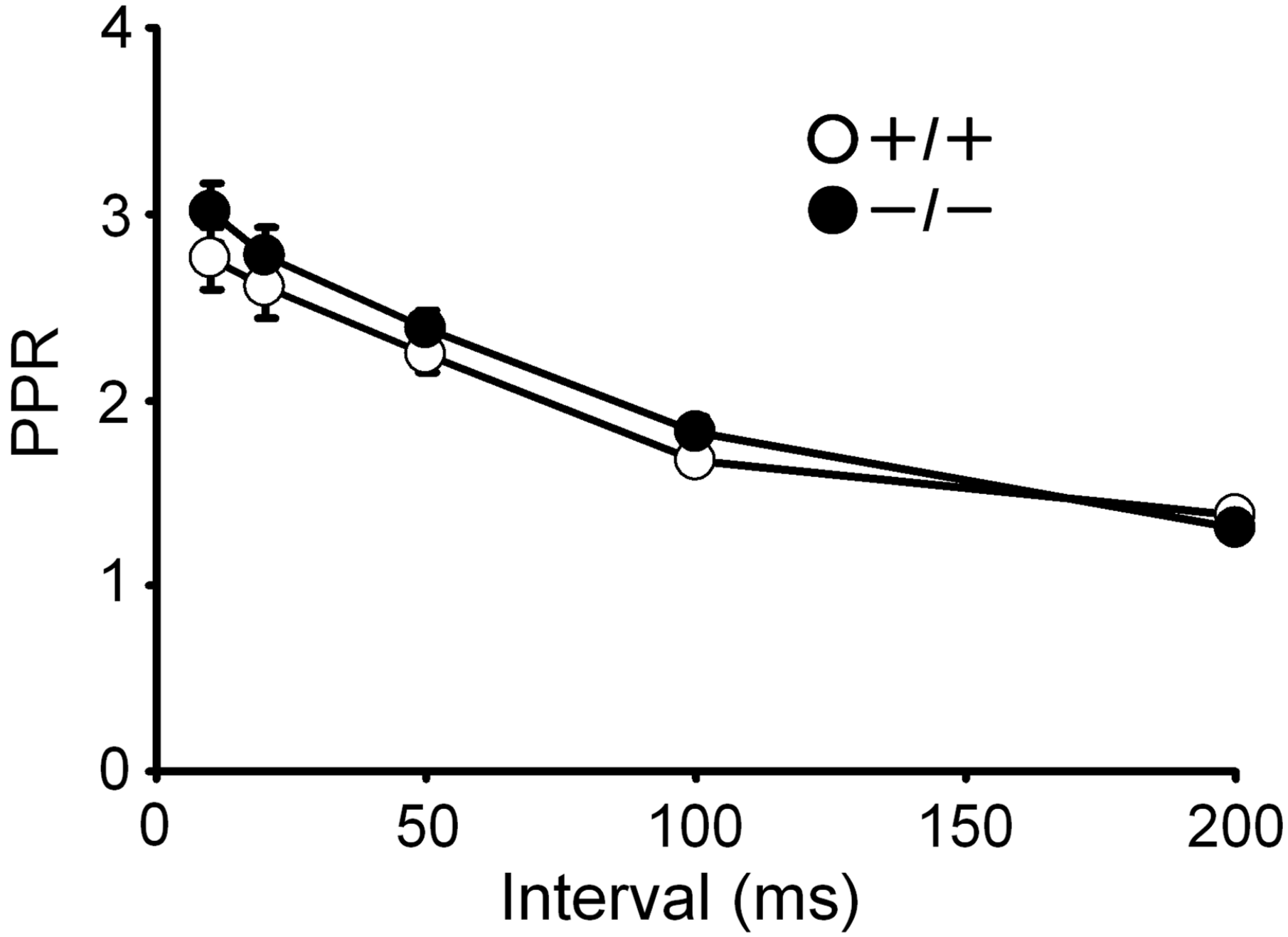

Supplemental Figure 3

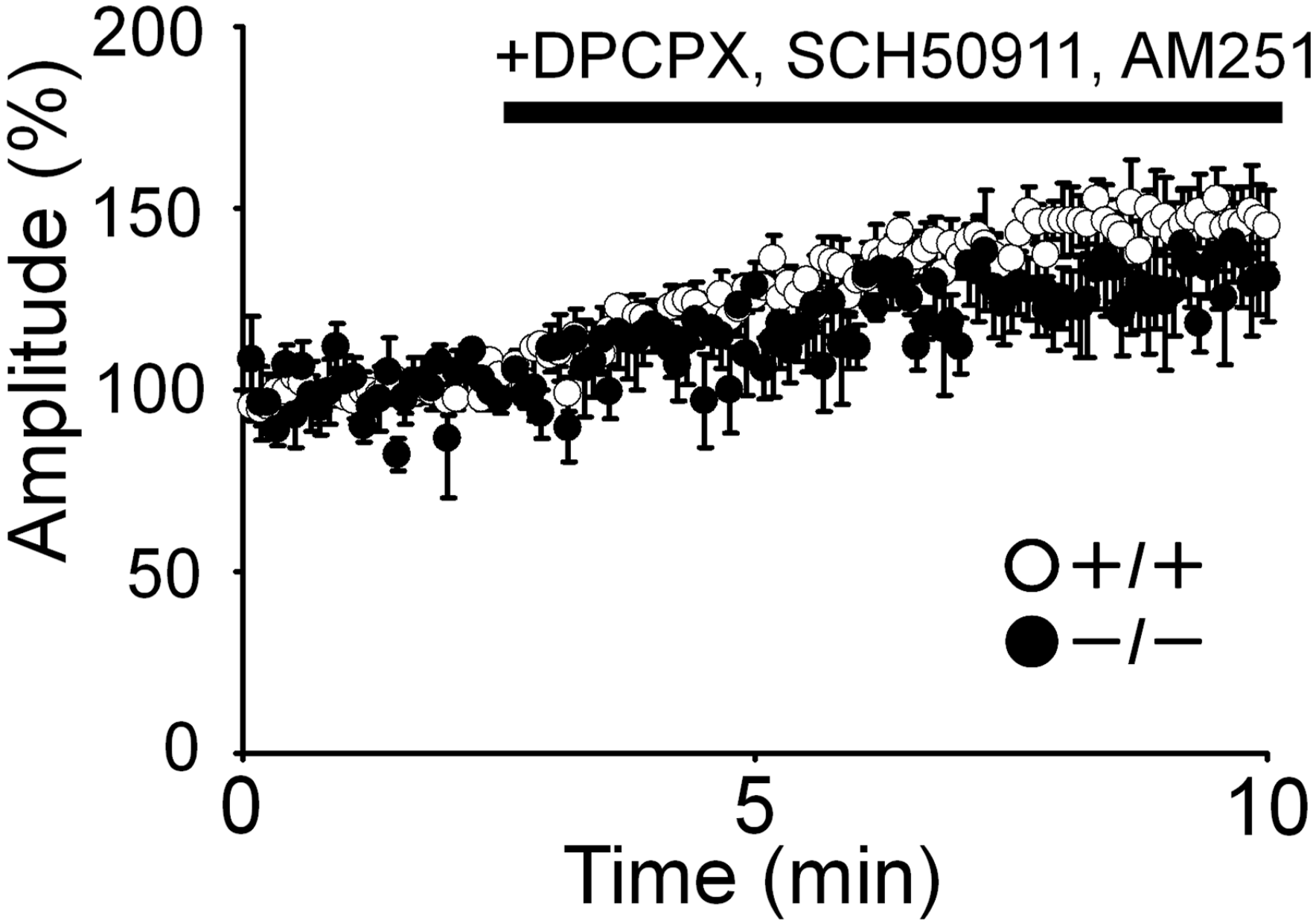

Supplemental Figure 4